

Technical report 19-010

A Pilot Protection Method Based on Energy Balance for Half-Wavelength Transmission Lines*

J. Fu, G. Song, and B. De Schutter

To cite this work, please refer to the published version:

J. Fu, G. Song, and B. De Schutter, “A pilot protection method based on energy balance for half-wavelength transmission lines,” *Proceedings of the 15th IEEE International Conference on Automation Science and Engineering (CASE 2019)*, Vancouver, Canada, pp. 18–23, Aug. 2019. doi:[10.1109/COASE.2019.8843110](https://doi.org/10.1109/COASE.2019.8843110)

Delft Center for Systems and Control
Delft University of Technology
Mekelweg 2, 2628 CD Delft
The Netherlands
phone: +31-15-278.24.73 (secretary)
URL: <https://www.dcsc.tudelft.nl>

* This report can also be downloaded via <https://dpub.eu/19-010>

A pilot protection method based on energy balance for half-wavelength transmission lines

Jianfeng Fu, Guobing Song, *Member, IEEE*, and Bart De Schutter, *Fellow, IEEE*

Abstract— When the current differential protection is applied to very long transmission lines such as half-wavelength transmission lines, it suffers from the distributed capacitive current as well as from low sensitivity in case of a high-resistance fault. In case of an external fault, the variation of the line storage energy, the distributed resistance energy loss, and the energy injected from both ends of the transmission line satisfy the energy balance equation, and in this case the energy balance is independent of the line length. However, in case of an internal fault, the energy dissipated by the fault resistance breaks the energy balance. Based on the theory of energy balances, this paper proposes a novel pilot protection principle. Compared with the existing long-distance transmission line protection principles, the proposed pilot protection principle has the advantage of not being influenced by the distributed parameters of the long line. A simulation based on EMTDC/PSCAD illustrates the benefits of the proposed approach.

Index Terms— pilot protection, energy balance, half-wavelength transmission lines, line protection, identification of high-resistance faults

I. INTRODUCTION

For a long time, the transmission of renewable energy has been a problem because of the usually far distance between renewable energy generation farms and load centers [1]. On the other hand, especially in recent years, intercontinental energy interconnection plans have been put forward by many scholars and intercontinental power transmission schemes have attracted a lot of interest [2-3]. A half-wavelength transmission line refers to a line whose transmission distance is 3000km long for a 50Hz frequency or 2500km long for a 60Hz frequency. Besides 3000km and 2500km lengths, using artificial tuning technology, the transmission distances can be designed in a wide range [4]. Half-wavelength transmission lines have the advantage that they do not require reactive power compensation devices, have excellent voltage stability and an extremely short electrical distance, and offer more economical benefits compared to EHVAC transmission lines [5].

The pilot protection is a protection based on the principle of comparison of specific data collected from two ends of transmission line. Pilot protection has been proposed

aiming to diagnose large resistance grounded faults in high-voltage large-capacity transmission lines [6]. Assessment in practical engineering projects shows that pilot protection is superior for the main protection of high-voltage transmission lines [7]. Therefore, pilot protection is important for ensuring the reliable operation of high-voltage transmission lines. However, the distributed parameters of half-wavelength transmission lines challenge the traditional pilot protection schemes, because of the non-negligible distributed capacitive current and a strongly non-linear distribution of currents and voltages along the line. Therefore, it is necessary to develop a new pilot protection principle that diagnoses the fault without reference to the length of the line. Furthermore, it is better to have a satisfactory sensitivity for high-resistance grounded faults.

At present, the protection of half-wavelength transmission lines is a topic of active research [8-12]. The paper [8] calculates the terminal current according to the Bergeron model, and builds the protection principle based on the difference between the sampled current and the calculated current. The paper [9] corrects the fault distance obtained by the distance measuring equation on the basis of the wave transmission law, but it does not consider the feasibility of the application to large-resistance grounded faults. According to [10] the differential current traveling wave protection of the power frequency is recommended compared with that of the time domain, because of the long distance and the skin effect of half-wavelength transmission lines. The paper [11] defines the false synchronization impedance to discriminate between internal and external faults. This kind of protection acts more quickly than traditional differential protection. The paper [12] proposes a scheme that takes the resistance into account and uses the power frequency component of the differential current to identify the fault so as to avoid the influence of the frequency-dependence of the line parameters.

Considering the difficulties due to negligible distributed capacitive currents and low sensitivity in fault discrimination for high-resistance grounded faults, the current paper utilizes the energy balance relationship among the net injected energy to the transmission line, the transmission line storage energy variation, and the transmission line resistance energy loss. Accordingly, a novel protection principle is developed, addressing the feasibility problem of protection of half-wavelength transmission lines and the difficulty of fault discrimination for large-resistance grounded faults. Apart from that, the computational burden of the new method will be low enough when applied into practice. Note that in this paper we do not consider directionality data, for that topic

* The research reported in this paper has been supported by the CSC (Chinese Scholarship Council).

Jianfeng Fu is with the Delft Center for Systems and Control in Delft University of Technology, Delft, The Netherlands. (e-mail: J.Fu-1@tudelft.nl)

Guobing Song is with the School of Electrical Engineering in Xi'an Jiaotong University, Xi'an, China. (e-mail: song.gb@163.com)

Bart De Schutter is with the Delft Center for Systems and Control in Delft University of Technology, Delft, The Netherlands. (e-mail: B.DeSchutter@tudelft.nl)

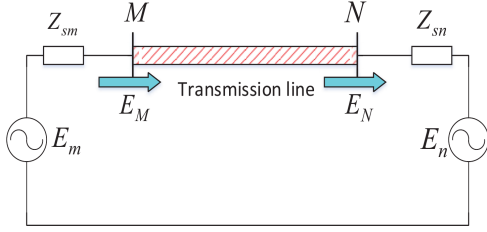


Fig. 1.a: Transmission line in normal operation

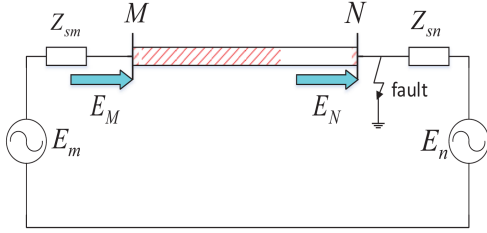


Fig. 1.b: Transmission line with external fault

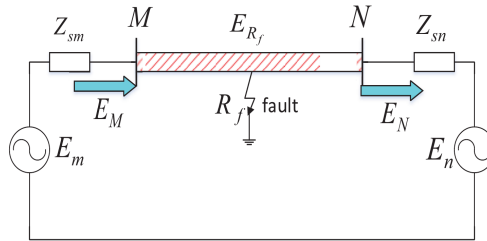


Fig. 1.c: Transmission line with internal fault

we refer the interested reader to [13, 14]

II. PROTECTION PRINCIPLE BASED ON THE ENERGY BALANCE

A typical half-wavelength transmission system is shown in Fig. 1. For a given time window the energy balance relation for normal operation (Fig. 1.a) as well as for an external fault (Fig. 1.b) is given by:

$$E_M - E_N - \Delta E_L - E_R = 0 \quad (1)$$

with E_M and E_N the total energy flowing through the M and N terminals. Moreover, ΔE_L is the difference in reserved energy¹ in the transmission line between the beginning and the end of the time window and E_R is the total energy loss consumed by the distributed resistance along the transmission line.

However, when an external fault occurs, as shown in Fig. 1.c, the energy balance relation becomes:

$$E_M - E_N - \Delta E_L - E_R = E_{Rf} \quad (2)$$

with E_{Rf} the energy consumed by the fault resistance.

From (1) and (2), it can be concluded that the difference between the variation of the energy stored in the transmission line and the net energy injected into the transmission line is

¹The reserved energy is the total energy reserved by the electric field and magnetic field along the line.

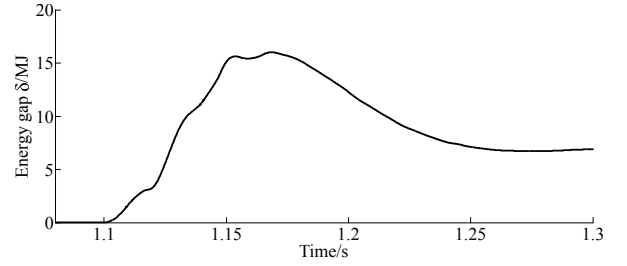


Fig. 2.a: Typical energy gap for an internal fault

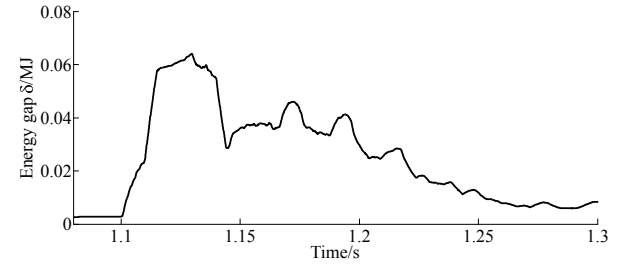


Fig. 2.b: Typical energy gap for an external fault

equal to the transmission line resistance energy loss both in normal operation or when an external fault occurs. However, in case of an internal fault, the difference is larger than the transmission line resistance energy loss. So, let us define a value δ such that:

$$\delta = |E_M - E_N - \Delta E_L - E_R| \quad (3)$$

Now the criteria for internal fault and external fault (or normal operation) can be described as:

$$\begin{cases} \delta \geq \delta_{set} & \text{(Internal fault)} \\ \delta < \delta_{set} & \text{(External fault)} \end{cases} \quad (4)$$

with δ_{set} a threshold value close to zero; this value should be selected based on the maximum unbalance energy gap when an external fault occurs. In this paper, the threshold value is selected as 1.2 times the maximum unbalance energy gap when an external fault occurs. Fig. 2 shows the energy gap of a typical internal fault and an external fault with the fault occurring at time instant 1.1s.

From Fig. 2, it is obvious that the δ value of an internal fault is far larger than that of an external fault. Therefore, the criterion (4) is effective to discriminate between internal faults and external faults.

III. CALCULATION OF THE CRITERION

By (3) the value of δ is based on the values of E_M , E_N , ΔE_L and E_R . Next, we first discuss how to compute ΔE_L and E_R (Section III-A) and next E_M and E_N (Section III-B).

A. Calculation of reserved energy and resistance loss

The time-varying reserved energy can be divided into two parts: the electric field energy of the distributed capacitor and the magnetic field energy of the distributed inductance. In this paper, we consider the calculation of the magnetic field energy in detail. As the electric field energy can be

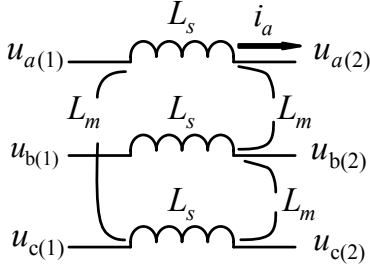


Fig. 3: Two-ports network of transmission line self-inductance and mutual-inductance

calculated in a similar way, the calculation of the capacitor reserved energy will not be discussed. It should be noted that the currents and voltages along the line are distance-varying. Firstly, the reserved energy calculation is based on a unit-length transmission line. According to electromagnetic field theory, the reserved energy of an inductance is equal to the energy absorbed from the 0 energy state to the steady state. Furthermore, in the actual model of the unit-length transmission line, the self-inductance and the mutual inductance are coupled as Fig. 3 illustrates. In this paper, to simplify the exposition, it is generally assumed that the self-inductances of the three phases are equal, and the three mutual inductances are also equal to each other.

In Fig. 3, L_s is the self-inductance of the unit-length transmission line; L_m is the mutual inductance of the unit-length transmission line; i_a, i_b, i_c are ABC phase currents; and $u_{abc(1)}$ and $u_{abc(2)}$ are the voltages at terminals 1 and 2 respectively. So, the voltage difference between two terminals and the power flow for phase A can be obtained as:

$$u_{a(1)} - u_{a(2)} = L_s di_a/dt + L_m di_b/dt + L_m di_c/dt \quad (5)$$

$$P_a = (u_{a(1)} - u_{a(2)})i_a \quad (6)$$

From (5) and (6), the reserved energy of the phase A inductance can be obtained as:

$$E_{La} = \int_t^{t+t_s} P_a dt = \int_t^{t+t_s} (L_s di_a + L_m di_b + L_m di_c)i_a \quad (7)$$

where t_s is the length of the time window that is used to smooth the sampling error. In this paper, a 10ms long time window is selected. Therefore, the reserved energy of the inductance of the unit-length transmission line is:

$$E_{Ll} = L_s(i_a^2 + i_b^2 + i_c^2)/2 + L_m i_a i_b + L_m i_a i_c + L_m i_b i_c \quad (8)$$

In a similar way, the reserved energy of the distributed capacitor of the unit-length transmission line is:

$$E_{C1} = \frac{1}{2}C_s(u_a^2 + u_b^2 + u_c^2) + C_m(u_a - u_b)^2 + C_m(u_a - u_c)^2 + C_m(u_b - u_c)^2 \quad (9)$$

The sum of (8) and (9) is the reserved energy of the unit-length transmission line. The distribution of voltages and currents along the transmission line can be calculated by M and N terminal currents and voltages according to

the Bergeron model [6]. After integrating or adding up all transmission line length units, the reserved energy of whole line can be obtained:

$$E_L = \int_t^{t+t_s} E_l dx = \int_t^{t+t_s} (E_{L1} - E_{C1})dx \quad (10)$$

The loss of transmission line resistance E_R is different from ΔE_L , as it is a value accumulating over time. More specifically, E_R can be obtained as

$$E_R = [R_s(i_a^2 + i_b^2 + i_c^2) + R_m i_a i_b + R_m i_a i_c + R_m i_b i_c]t_s \quad (11)$$

B. Calculation of the energy gap

Based on the calculation of the reserved energy and the transmission line loss, the energy gap δ in (3) can be obtained:

$$\delta = \left| \int \sum_{p=a,b,c} (u_{Mp} i_{Mp} + u_{Np} i_{Np}) t_s dt - \Delta E_L - E_R \right| \quad (12)$$

where $(u_{Mp} i_{Mp} + u_{Np} i_{Np}) t_s$ is the net energy that is flowing through phase p (p can be A, B, or C) of the transmission line over a time window period t_s . On one hand, using voltages and currents of the M terminal, a pair of E_R and ΔE_L values can be calculated. On the other hand, using the voltages and the currents of the N terminal, another pair of E_R and ΔE_L values can be calculated. Therefore, two energy gaps can be obtained, respectively represented by the symbols δ_M and δ_N .

When an internal fault occurs at the terminal of the transmission line, e.g. the M terminal, the voltages and currents along the transmission line can be determined from the voltage and the current of the M terminal, but nearly all the voltages and currents will be inaccurate. That implies that we will have a large δ_M . On the contrary, the voltages and currents along the transmission line obtained from the voltage and the current of the N terminal are quite accurate. That implies a small δ_N . So, the maximum value of δ_M and δ_N can be applied in criteria in order to discriminate between the terminal faults. Hence, we set

$$\delta = \max\{\delta_M, \delta_N\} \quad (13)$$

So, the threshold value δ_{set} should be set according to the maximum value among four values: δ_M and δ_N of an external extreme fault at the M terminal as well as δ_M and δ_N of an external extreme fault at the N terminal so that the threshold condition is not triggered for an external fault or in case of normal operation.

IV. SIMULATION RESULTS

Now a case study involving a half wave-length transmission line is considered to illustrate the advantages of the proposed approach.

A. Parameters of the case study

Based on the EMTDC/PSCAD platform, the simulation mode of a 750kV, 50Hz, 3000km long single circuit transmission line is built. The structure of the transmission line towers

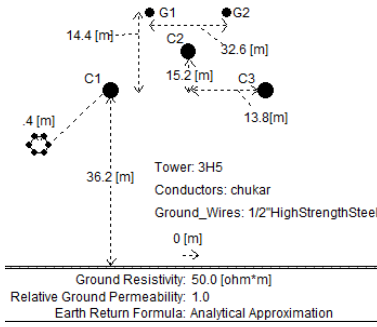


Fig. 4: The tower structure model in PSCAD [13]

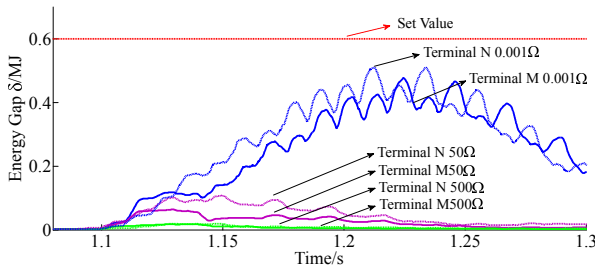


Fig. 5: Considered cases of external three-phase grounded faults

which decide the transmission line parameters is shown in Fig. 4 [15]:

Besides the parameters shown in Fig. 4, the geometric mean radius of the conductor is 0.0112m, the sags for all conductors are 18.2m, the ground wire radius is 0.00575m, the ground wire resistance is 2.13 Ω /km, and the sags of all grounded wires are 12.6m. The above parameters can be transformed into unit-length transmission line parameters as described in [16].

B. Simulation results and sensitivity analysis

In this paper, the PSCAD simulation platform is used to obtain the energy gaps to verify the effectivity of the proposed protection principle by a large number of simulations. Several representative simulation results are selected to illustrate the operational characteristics of this protection principle. It should be noted that the time axis of the simulation plots does not take transmission delay into account, i.e., the actual action time is the sum of action time instant in the plot and the time needed for data transmission to the opposite terminal.

Fig. 5 shows typical energy gap curves for external faults at the M and N terminals. It can be seen from the figure that the energy gap δ is very small. Furthermore, as the value of the fault resistance decreases, the energy gap increases. Therefore, the threshold value can be given as 1.2 times the maximum energy gap of the three-phase external metallic fault, which has a fault resistance value approximately equal to zero. In this paper, the threshold value is taken as $\delta_{set} = 0.6\text{MJ}$.

Fig. 6 shows the simulation result of a three-phase grounded fault occurring 500km from the terminal M for

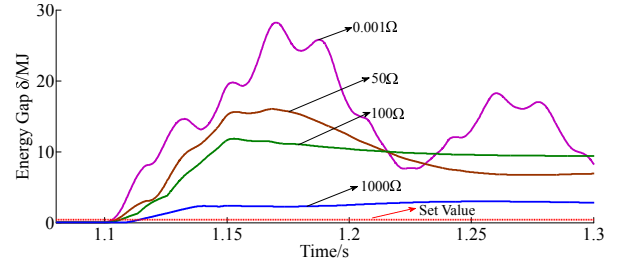


Fig. 6: Considered cases of internal faults occurring 500km away from the M terminal with different fault resistances

different fault resistances. Several fault characteristics of this protection principle can be clearly seen from the figure:

- During an internal fault period, when the voltages and currents along the line are calculated based on the voltages and currents of terminal M , it is difficult to accurately calculate the distribution of the voltages and currents between the fault point and the terminal N because of the traveling wave refraction on the fault point. In other words, we can calculate the current and the voltage distribution accurately and the error δ is lower than δ_{set} when an external fault occurs or in case of normal operation. But we cannot calculate the distribution accurately when an internal fault occurs because of the refraction of the traveling wave. Then, the error δ will be larger than δ_{set} . The inaccuracy increases the energy gap δ and also makes the δ value fluctuate more strongly, which is beneficial to protection actions as shown in (4).
- The fault transient period becomes shorter as the fault resistance increases.
- At a given fault location, as the fault resistance increases, the action speed of the protection scheme will slow down. However, a large number of simulation results show that, in the cases of low-or-medium-fault resistances, the protection has an action speed less than 10ms.

Fig. 7 shows the simulation results for various types of faults with a fault resistance of 1000 Ω occurring at the lowest voltage point along the line. Comparing Fig. 6 and Fig. 7, it can be seen that the closer the fault point is to the lowest point of the voltage, the smaller the energy gap δ will be. This is because when the fault occurs at the lowest point of the voltage, the severity of the fault is lowest, and the calculation inaccuracy of the voltages and currents along the line is greatly reduced. Therefore, the sensitivity is the lowest in this case.

Since the single-phase grounded fault has the lowest severity among the considered fault types, it can be inferred that the sensitivity of the high-resistance single-phase grounded fault at the lowest voltage point is the lowest. So for faults with fault resistances up to 1000 Ω , the protection principle still has a sufficient sensitivity.

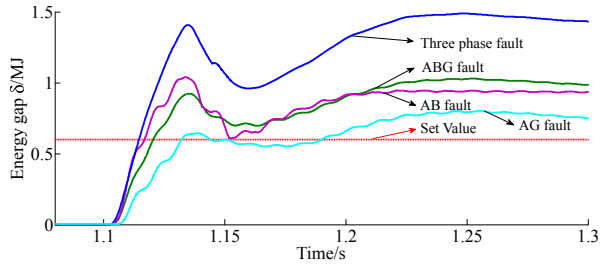


Fig. 7: Considered cases of internal faults at the lowest voltage spot (ABG means that the A phase, the B phase, and the ground are connected).

TABLE I: Maximum energy gap for different fault time instants

Fault time instant [s]	1.100	1.102	1.104	1.106	1.108	1.110
δ [MJ]	3.23	3.224	3.222	3.22	3.129	3.126
Fault time instant [s]	1.112	1.114	1.116	1.118	1.120	
δ [MJ]	3.129	3.22	3.222	3.224	3.23	

C. Influence of the fault time instant

Now we fix a constant fault location, fault type, and fault resistance, and we explore the impact of different fault time instants on the protection sensitivity. The selected fault location is 500km from the terminal M . In addition, the fault type is a single-phase grounded fault, and the fault resistance is 100Ω . Because the transmission frequency of electric power is 50Hz and periodic, we select fault time instants every 0.002s so that there are 10 time instants in 20ms cycle. After the simulations on the platform of PSCAD, the energy gap peaks for different fault time instants are listed in Table 1 below.

It can be seen from Table I that the fault moment has little effect on the pilot protection proposed in this paper, and basically does not affect the action judgment and action time of the protection.

D. Influence of the transmission power

The transmission power often affects the discrimination result of the protection operation. Considering the half-wavelength transmission line under a transmission power that is larger than the regular power level, there will be a voltage distribution characteristic of low voltages at both terminals and a high voltage at the midpoint of the line. This causes a cost increment for insulation of the electrical equipment. Thus, in practice the transmission power of the transmission line will not exceed the regular power level too much. On the other hand, a transmission power below the regular power level will lead to a poor line utilization. Therefore, this paper only considers variations of the transmission power of a half-wavelength transmission line in the vicinity of the regular

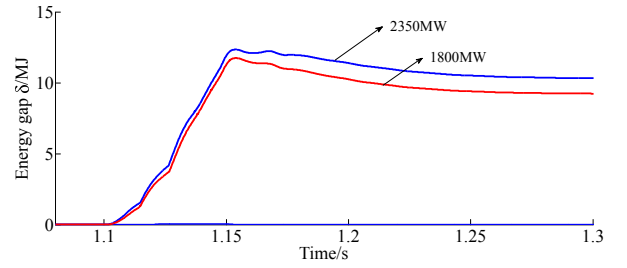


Fig. 8.a: Influence of transmission power for internal faults

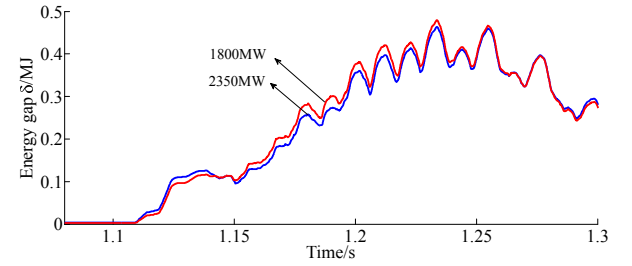


Fig. 8.b: Influence of transmission power for external faults

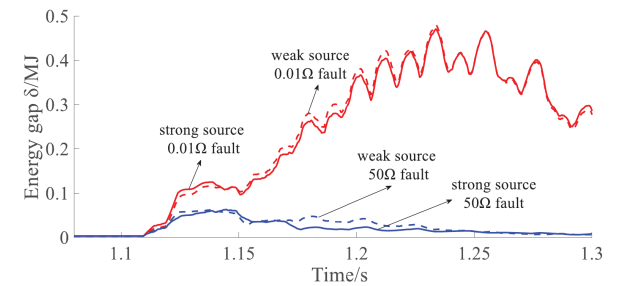


Fig. 9: Influence of source strength for external faults

power level. Fig. 8.a and Fig. 8.b present the simulation results of three-phase metallic external faults and three-phase internal grounded faults with a fault resistance of 100Ω at the location 500km away from terminal M .

Fig. 8.a and Fig. 8.b shows impact effect of transmission power for internal faults and external faults respectively. It can be seen that the transmission power variation has a very weak influence in the case of an external fault, and a limited impact for the internal fault. This shows that the transmission power variation has an effect on the protection sensitivity, but the effect on the protection threshold is very small. When an internal fault occurs, as the transmission power decreases, the protection sensitivity decreases, and the energy gap becomes smaller, but these changes have little effect on the final fault diagnosis result.

E. Influence of the strength of the source

Fig. 9 and Fig. 10 show the influence of external faults and internal faults (of 0.01Ω and 50Ω) under a weaker source of $5+43j\Omega$ (dashed line) and a stronger source of $2.5+21.5j\Omega$ (solid line).

From Fig. 9, obviously, the strength of the source has little effect on the protection behavior under external faults as the differences between the dashed and the solid lines are

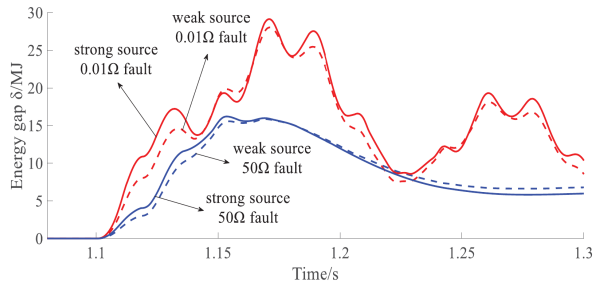


Fig. 10: Influence of source strength for internal faults

small. Thus, the strength of the source has little effect on the threshold value.

From Fig. 10, similarly, the strength of the source has little effect on the protection behavior under internal faults as the differences between the dashed and the solid lines are small. Thus, the strength of the source has little effect on the internal fault discrimination. Thus, we can conclude that the strength of power source has a little influence on the behavior of protection.

V. CONCLUSIONS

This paper introduces a novel pilot protection principle for high-impedance grounded faults in long transmission lines. The principle uses the time domain voltages and currents at both terminals of the line to derive the distribution of voltages and currents along the line, thereby calculating the energy stored in the line and the energy losses. The protection criterion is then constructed based on the energy balance equation. The principle can be applied to half-wavelength transmission lines, and offers the advantages of being free from the influence of distributed line capacitance, good recognition capability of high-resistance grounded faults, being free from the fault time instant, free from transmission power, free from the strength of the source, and being easy to implement in practice.

REFERENCES

- [1] F. Iliceto, E. Cinieri, "Analysis of half-wavelength transmission lines with simulation of corona losses," *IEEE Transactions on Power Delivery*, vol.3(4), pp. 2081-2091, October 1988.
- [2] Y. Zhang, Z. Zhang, Y. Zhang, "Application research on UHVDC technology in asia-Europe power transmission planning," *Power System Technology*, vol. 39(8), pp. 2069-2075, 2015.
- [3] Z. Liu, "Research of global clean energy resource and power grid interconnection," *Proceedings of the CSEE*, vol.36(19), pp. 5103-5110, 2016.
- [4] G. Wang, Q. Li, L. Zhang, "Research status and prospects of the half-wavelength transmission lines," 2010 Asia-Pacific Power and Energy Engineering Conference, April 2010.
- [5] D. Santos, A. Jardini, P. Casolari, R. Vasquez-Arnez, G. Saiki, T. Sousa, G. Nicola, "Power transmission over long distances: economic comparison between HVDC and half-wavelength line," *IEEE Transactions on Power Delivery*, vol. 29(2), pp. 502-509, August 2013.
- [6] S. Gao, J. Suonan, G. Song, J. Zhang, Z. Jiao, "Fault location method for HVDC transmission lines on the basis of the

distributed parameter model," *Proceedings of the CSEE*, vol. 30(13), pp. 75-80, 2010.

- [7] B. Wang, X. Dong, Z. Bo, A. Klimek, "Negative-sequence pilot protection with applications in open-phase transmission lines," *IEEE Transactions on Power Delivery*, vol. 25(3), pp:1306-1313,2010.
- [8] S. Xiao S, Y. Cheng, W. Wan, Y. Wang, "Relay protection for half wavelength AC transmission line," *IEEE International Conference on Advanced Power System Automation and Protection (APAP 2011)*, pp. 1308 - 1311, 2011.
- [9] F. Lopes, B. Küsel, K. Silva, "Fault location on transmission lines little longer than half-wavelength," *Electric Power Systems Research*, vol. 114(3), pp. 101-109, 2014.
- [10] L. Tang, X. Dong, "Study on the characteristic of travelling wave differential current on half-wave-length AC transmission lines," *Proceedings of the CSEE*, vol. 114(3), pp. 101-109, 2017.
- [11] Z. Zhou, H. Liu, Y. Guo, D. Du, D. Wang, "The false synchronization differential protection for half-wavelength transmission line," *Proceedings of the CSEE*, vol. 36(24), pp. 6780-6787, 2016.
- [12] L. Tang, X. Dong, "A travelling wave differential protection scheme for half-wavelength transmission line," *International Journal of Electrical Power & Energy Systems*, vol. 99, pp. 376-384, 2018.
- [13] L. Aoyu, D. Xinzhou, F. Teng, et al., "Study of fault direction characteristic of half-wave-length AC transmission lines," *Power System Technology*, vol. 12, pp. 103-110, 2017.
- [14] G. Benmouyal, J. Mahseredjian, "A combined directional and faulted phase selector element based on incremental quantities," *Power Engineering Review*, vol. 21(8), 2001.
- [15] X. Fu, D. Ju, G. Li, "The calculation of 750kV line parameters based on ATP-EMTP simulation," *IEEE International Symposium on Computer, Consumer and Control*, pp. 160-163, 2016.
- [16] R. Marti, "Accurate modeling of frequency-dependent transmission Lines in electromagnetic transient simulations," *IEEE Transactions on Power Apparatus & Systems*, vol. PAS-101(1), pp. 147-157, 1982.